

Dynamics of low-energy-electron stimulated desorption of metastable particles from N₂ condensed on Xe and Kr films

H. Shi, P. Cloutier, J. Gamache, and L. Sanche

Groupe du Conseil de Recherches Médicales en Science des Radiations, Faculté de Médecine, Université de Sherbrooke, Sherbrooke, Quebec, Canada J1H 5N4

(Received 13 November 1995)

Electron-impact desorption of metastable molecular nitrogen (N₂^{*}) from N₂ condensed on Xe or Kr multilayer films is investigated as a function of electron energy (0–70 eV), rare-gas film thickness, and N₂ coverage. The different behaviors are explained with a simple mathematical expression which takes into account the parameters influencing the magnitude of the desorption yields. Two basic mechanisms are identified to contribute to the observed N₂^{*} yields: the direct excitation and electronic energy transfer. The former mechanism proceeds via electronic excitation of adsorbed N₂ by the primary electron beam followed by exciton motion to the surface and desorption. In the energy-transfer mechanism, primary electrons first create excitons in the rare-gas films which then transfer their energy to the adsorbed N₂ molecules. N₂^{*} desorption at the N₂-film-vacuum interface can proceed via intramolecular to molecule-surface bond vibrational energy exchange and via cavity expulsion. When energy transfer dominates desorption, the N₂^{*} yield function clearly bears the characteristics of exciton creation in the rare-gas film. The relative contributions of these two mechanisms depend on the impact electron energy, and layer thickness of N₂ and rare-gas film. The different energy-transfer efficiencies between excited rare-gas atoms and N₂ molecules is found to be the major cause for the observed difference in N₂^{*} yield between the Xe and Kr film substrates. [S0163-1829(96)05920-6]

I. INTRODUCTION

The interaction between electronically excited solids and adsorbed molecular species has been demonstrated to have significant potential for the selective modification of solids and adsorbate system.^{1–3} Investigations of the nature of the initial excitation and the nature of the coupling between the solid and the adsorbed species can provide an understanding of energy deposition, transport, and trapping processes in the solid phase. Elementary processes in DIET (desorption induced by electronic transitions) include primary excitation, evolution of electronic excitation (propagation, localization, and on-site evolution like Auger decay, etc.) and coupling of the electronic excitation to nuclear motion.⁴ The study of the desorption phenomenon in double-layer films is expected to provide information on these elementary processes. Electron impact may induce primary excitations of the species in such targets, and the evolution of the electronic excitation may include various possible excitation-energy transfer and decay processes.

The excitation and relaxation processes in rare-gas (RG) solids are presently quite well understood.^{5–7} The energy is initially deposited via creation of a free exciton or free-electron-hole pairs. Relaxation pathways include radiative decay⁸ and nonradiative quenching,^{9,10} as well as trapping in a dimer or an atomic configuration. Different options for trapping modalities (molecular and atomic self-trapped excitons) and sites (imperfections, impurities, and surface) lead to a rich spectrum of vacuum-ultraviolet luminescence.^{5–13} The trapping and localization of excitons are essential to desorption.^{6,7} These processes are very sensitive to surface conditions, and the desorption and luminescence features are modified by adding foreign atoms or molecules to RG solids.^{14,15}

While desorption of species in long-lived electronically excited states (i.e., metastable species) only accounts for a small fraction of the desorbed particles, it provides the possibility for isolating particular processes of importance in understanding DIET. Stimulated metastable-particle (MP) desorption has been observed from condensed RG solids.^{10,12,16–20} The desorption mechanism is believed to be cavity expulsion,¹⁰ which suggests that the excited atom or molecule located at the surface experiences a repulsive interaction with all neighbors if the matrix has a negative electron affinity, and this repulsive potential propels the excited species into vacuum. Inside the bulk, this repulsion leads to the formation of a cavity around the excited particle. In crystals with a positive electron affinity, the excited particle is not expelled owing to the attractive interaction of the excited-orbit electron cloud with the neighbor atoms. Quantitative calculations²¹ were able to predict details of the Ar^{*} desorption¹⁹ and the absence of cavity expulsion of Kr^{*} from Kr crystals (Kr and Xe have a positive bulk electron affinity⁶).

Recently, we observed MP desorption from condensed N₂ and CO films.²² MP desorption thresholds lie at energies of 7.2 and 11.5 eV for excitation of the $B^3\Pi_g$ and $E^3\Sigma_g^+$ states of N₂, respectively. For CO, the MP desorption threshold at 8.0 eV is due to the formation of the vibrationally excited $a'^3\Sigma^+$ state.²² Desorption of N₂^{*} above 11 eV arises from the repulsive interaction of N₂^{*} with the solid matrix (i.e., cavity expulsion), while desorption of N₂^{*} below 11 eV and CO^{*} is due to the transfer of internal vibrational energy to the molecule-surface bond.²² Desorption induced by a monochromatic electron beam in double-layer films containing a multilayer of Xe onto which a single layer of the diatomic molecules N₂ and CO was condensed has been investigated by Mann *et al.*²³ The desorbed species were found to be N₂^{*}

and CO^* . The results showed an electron-energy dependence of the MP signal (i.e., a yield function) which resembled that for UV photons from a pure Xe film, indicating that the desorption of N_2^* and CO^* is mainly a bulk-mediated process.²³ It was proposed that the MP desorption is induced by an energy-transfer mechanism:²³ Xe bulk excitons are excited, and carry the initial excitation energy to the molecule-atom interface. There a diatomic molecule can be excited by an energy transfer from the Xe substrate as a result of a ‘‘collision’’ between a Xe exciton and the adsorbate molecule, similar to gas-phase excitation energy transfer. The desorbed metastables were considered to be vibrationally excited $\text{N}_2(B^3\Pi_g)$, $\text{CO}(a'^3\Sigma^+)$, and $\text{CO}(d^3\Delta)$.²³ Having lifetimes of several μs ,²⁴ the $\text{N}_2(B)$, $\text{CO}(a')$, and $\text{CO}(d)$ are sufficient long lived to desorb via vibrational energy transfer.^{25–28} They in turn decay to the lowest excited states $\text{N}_2(A^3\Sigma_u^+)$ and $\text{CO}(a^3\Pi)$, respectively, on their way to the detector.

While experiments with pure N_2 and CO films²² clearly showed that direct excitations induced by the electron beam lead to desorption of N_2^* and CO^* , the results from experiments on Xe films covered with one monolayer of N_2 and CO (Ref. 23) suggest that the energy-transfer mechanism dominates the stimulated MP desorption in this double-layer system. Nevertheless, direct desorption should also be present. The present work concentrates on the N_2 molecule and investigates N_2 -covered Xe and Kr films in an effort to understand the dynamics of MP desorption in such systems. Experiments are performed on the thickness dependence of both the N_2 and RG films within an extended electron-energy range. To understand the magnitude of the MP yields related to N_2 thickness in double-layer systems, we further perform a thickness-dependent experiment on pure N_2 films. A simple model is developed to explain the experimental results. While the information obtained with Xe films at very low electron energies corroborates the previous hypothesis of Mann *et al.*,²³ we find that on covered Kr films the energy-transfer mechanism alone cannot explain our observations even in the threshold region. Direct desorption is also involved. The relative contribution of the two processes (direct excitation and energy transfer) depends on the impact electron energy and layer thickness of N_2 and rare-gas films. Different energy-transfer efficiencies between excited rare-gas atoms and N_2 molecules are found to be responsible for the observed difference in N_2^* yields between the Xe and Kr substrate films.

II. EXPERIMENT

The experiment was performed in an ultrahigh-vacuum system reaching a base pressure of $\sim 10^{-10}$ Torr. The apparatus has been described in detail previously.¹⁹ Briefly, a well-collimated low-energy (1–70 eV) electron beam impinges on a Pt(111) single crystal at 18° with respect to the surface normal; the induced UV luminescence and desorbed metastable particles are measured with a large-area micro-channel plate array which is superimposed on a position-sensitive anode. The electronic energy threshold for the detection of metastable particles is estimated to lie around 6 eV.¹⁹ The electron beam has an intensity of 1 nA which is independent of electron energy in the range 5–70 eV; its

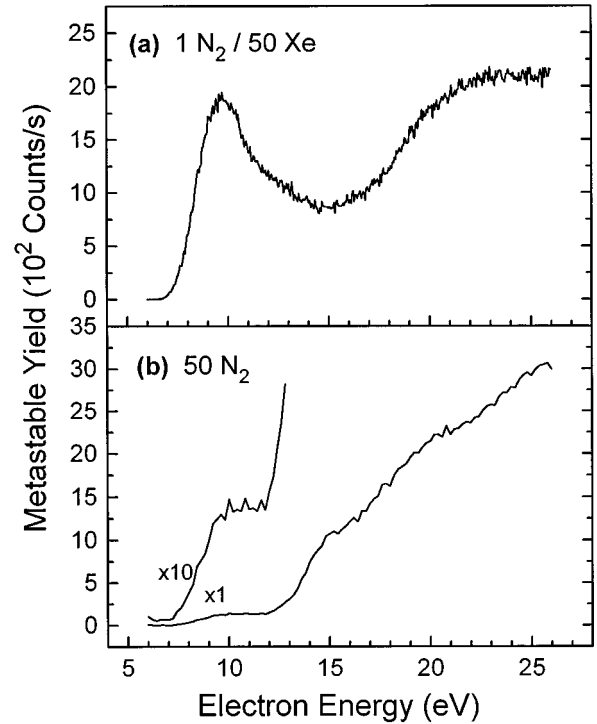


FIG. 1. (a) Metastable molecular nitrogen (N_2^*) desorption yields induced by 5–26-eV electron impact on a 50-monolayer (ML) Xe film covered by 1 ML of N_2 ($1\text{N}_2/50\text{Xe}$, reproduced from Ref. 23). (b) Same MP desorption yield function for a pure 50-ML N_2 film.

energy resolution is 60-meV full width at half maximum. The energy of the vacuum level is calibrated ± 0.3 eV by measuring the onset of the target current as the voltage between the electron source and the target is slowly increased. The crystal, which is mounted on the tip of a closed-cycle helium cryostat, can be cooled to 20 K and cleaned by electrical heating and Ar bombardment. The target films are grown on the Pt(111) surface by condensing from the vapor-phase Xe, Kr, and N_2 gases. These were supplied by Matheson of Canada Ltd. with a purity of 99.9995%. The thickness of a film is estimated from the amount of gas introduced and the quantity required to build the first monolayer (ML) as inferred from temperature-programmed desorption.¹⁹ The reproducibility of the film thicknesses is estimated to be $\pm 10\%$.

III. RESULTS

A. MP desorption from N_2 layers condensed on Xe films

In Fig. 1, the MP desorption yield function from 1-ML N_2 condensed on 50 ML of Xe ($1\text{N}_2/50\text{Xe}$, reproduced from Ref. 23) is compared to that from a pure N_2 film of 50 ML. The yield function from 50-ML N_2 [Fig. 1(b)] is similar to that published in Ref. 22, recorded for incident electron energies between 5 and 19 eV. Two regions of large intensity difference can be seen in Fig. 1(b), with thresholds at 7.2 and 11.8 eV, respectively, in agreement within the limits of the experimental error with previous results.²² According to the latter,²² the MP signal between 7.2 and 11.8 eV in Fig. 1(b) can be assigned to the excitation and desorption of the $B^3\Pi_g$ state of N_2 , and that above 11.8 eV to the $E^3\Sigma_g^+$ state of N_2 , respectively. For $1\text{N}_2/50\text{Xe}$ [Fig. 1(a)], the yield function

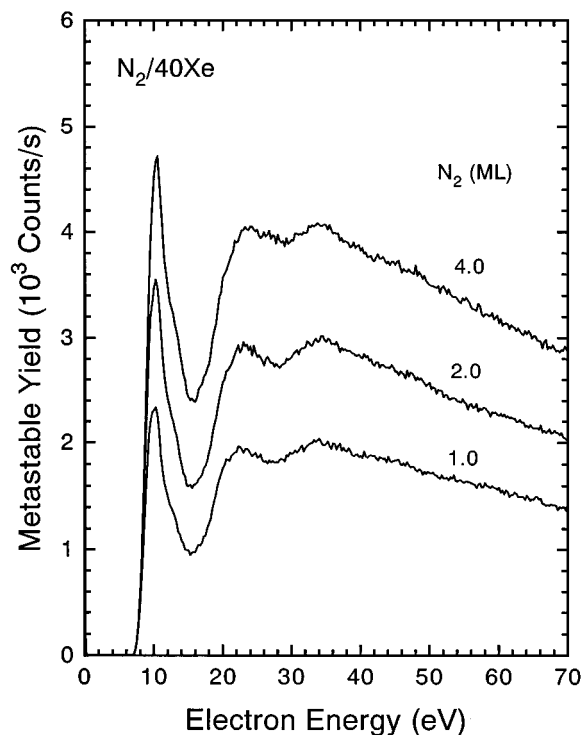


FIG. 2. N_2^* desorption yields induced by 0–70-eV electron impact on a 40-ML Xe film covered by various amounts of N_2 .

exhibits a threshold around 7.0 eV followed by a peak with its maximum at 9.8 eV. After a decrease in signal, the MP yield increases again, starting at an energy of 16 eV. A strong resemblance has been observed between the MP desorption yield function from $1N_2/50Xe$ and the luminescence yield from a pure Xe film (not presented here, see Ref. 16 and 23). From this comparison, it was proposed that N_2^* desorbs in the $B^3\Pi_g$ state from $1N_2/50Xe$ via the energy-transfer mechanism.²³ It is obvious in Fig. 1 that the yield functions from $1N_2/50Xe$ and 50-ML N_2 bear different characteristics, indicating the existence of different desorption mechanisms. In these two systems, N_2^* was the only metastable species produced.^{22,23}

In the N_2/Xe systems studied here, time-of-flight (TOF) distributions of the desorbed MP are observed to be the same as those for the $1N_2/50Xe$ system previously studied,²³ which were found to have a maximum at $44 \pm 5 \mu s$, and are interpreted to be due to metastable molecular nitrogen. The present MP yields are therefore also interpreted as due to N_2^* . No MP desorption is observed from pure multilayer Kr and Xe films.

The N_2^* yield dependence on the thickness of adsorbed N_2 on Xe films are shown in Figs. 2 and 3, for electron energies in the extended range 0–70 eV. These results were obtained from films prepared by condensing various amounts of N_2 on a 40-ML Xe film condensed on the Pt(111) surface. The overall magnitude of the signal increases with N_2 thickness. For 1, 2, and 4 ML of N_2 (Fig. 2), the N_2^* yield function bears the same characteristics. The desorption threshold is observed around 7.0 eV, and three peaks are observed at 10.3, 23, and 35 eV whose widths increase and whose amplitudes diminish with increasing energy. These characteristics favor assignment of the three peaks to excitation of one,

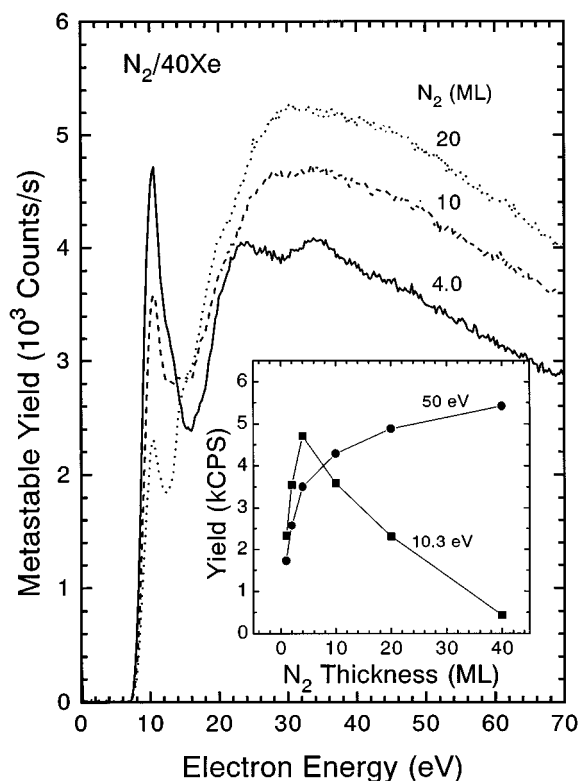


FIG. 3. N_2^* desorption yield function from a 40-ML Xe film covered by various amounts of N_2 . Inset: MP signals at 10.3 and 50 eV (taken from the yield function curves) as a function of N_2 thickness, kCPS refers to 10^3 counts/s.

two, and three excitons in Xe, respectively, due to multiple inelastic scattering of electrons. It implies that Xe^* transfer plays an important role for impact energy up to at least 35 eV.

For N_2 thickness greater than 4 ML (Fig. 3), the peak at 10.3 eV decreases considerably with N_2 thickness. However, the signal between 16 and 70 eV increases further and becomes a structureless curve of higher intensity between 30 and 40 eV. For 40-ML N_2 on 40-ML Xe (not shown), the peak at 10.3 eV vanishes, and the MP desorption yield function curve resembles that of a pure condensed N_2 film. The different trend for the two impact energy regions is demonstrated in the inset in Fig. 3 by a plot of the signals at 10.3 and 50 eV as a function of N_2 thickness. The data for $40N_2/40Xe$ are also used in the inset. While the intensity at 50 eV continually increases with N_2 thickness, the signal at 10.3 eV increases to a maximum at 4-ML N_2 and decreases rapidly with higher N_2 thickness.

In Fig. 4, the N_2^* yield dependence on the thickness of N_2 adsorbed on a 26-ML Xe film is shown in greater detail. The impact energies of 10.0 and 24.0 eV are chosen to obtain strong desorption yields [see Figs. 1(a) and 2]. The MP yield increases more or less linearly up to 3 ML of N_2 . A maximum lies at about 4.4 ML for an incident energy of 10 eV while for 24 eV a plateau is reached.

The N_2^* yield as a function of the thickness of the Xe film is shown in Fig. 5. It increases rapidly with the thickness of the Xe film, and saturates at 3 ML of Xe.

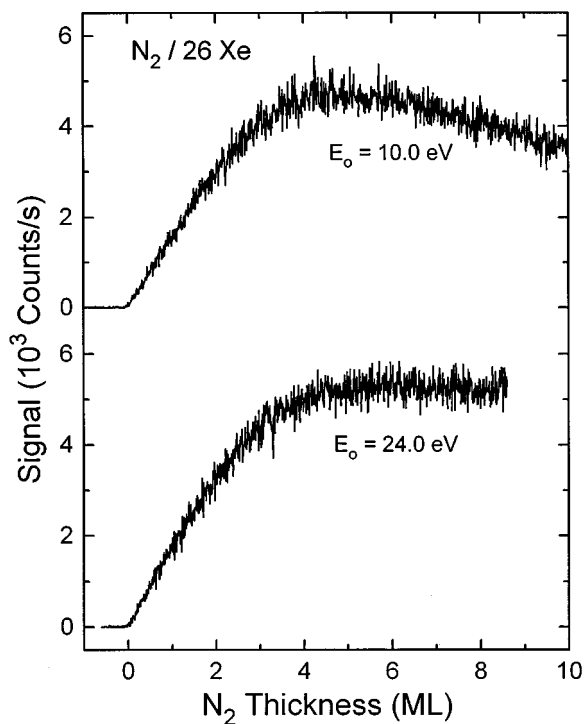


FIG. 4. The dependence of N_2^* desorption yield on the thickness of the adsorbed N_2 layers for N_2 adsorbed on a 26-ML Xe film, and electron-impact energies of 10.0 and 24.0 eV.

The thickness dependence of the N_2^* yield function from pure N_2 films is shown in Fig. 6. The semilogarithmic curves are similar in shape for various N_2 thicknesses. Analysis of the data in Fig. 6 indicates that within the 20–70 eV range the signal increases more or less linearly with N_2 thickness between 2 and 5 ML; above 5 ML, the rate of increase reduces gradually with a tendency toward saturation above 20

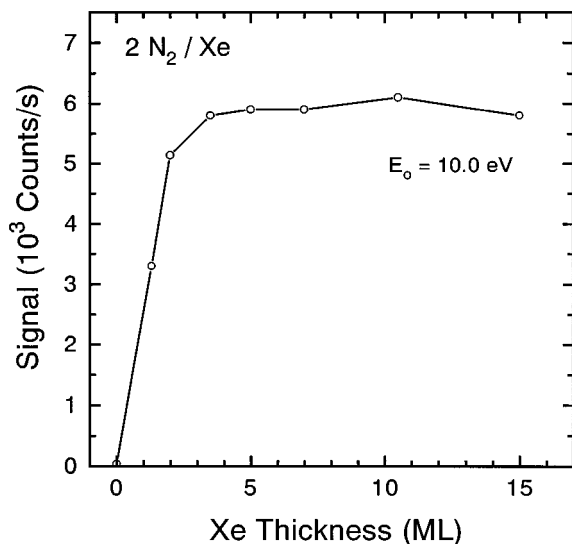


FIG. 5. The N_2^* desorption yield for 10-eV impact energy, as a function of the thickness of Xe space layers. 2 ML of N_2 were condensed on each Xe film.

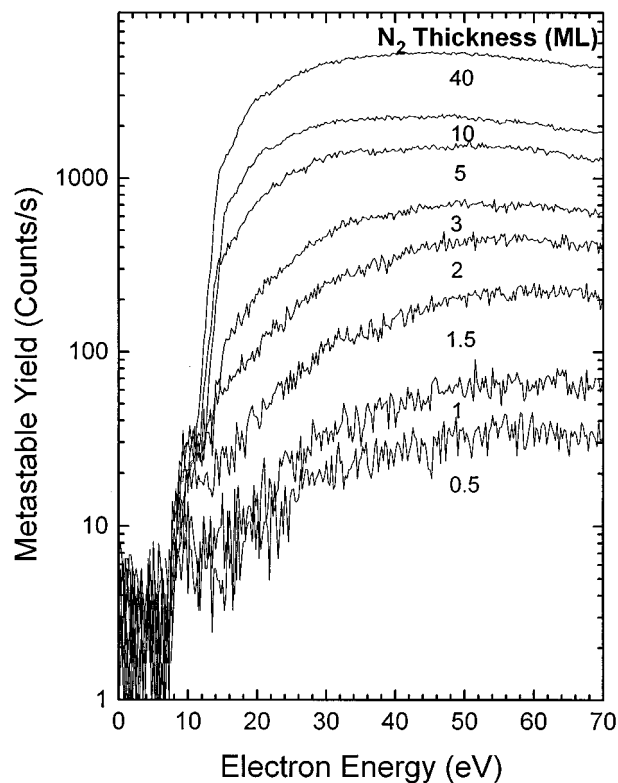


FIG. 6. Semilogarithmic N_2^* desorption yield functions for N_2 films of different thicknesses.

ML. Examples of these behaviors are given in Fig. 7 for incident energies of 24 and 50 eV.

B. MP desorption from N_2 layers condensed on Kr films

As in the case of N_2 /Xe double-layer films, TOF distributions of the desorbed MP signal from N_2 /Kr systems indicate that the desorbed species is N_2^* . The results reported in this section are therefore interpreted to be due to metastable molecular nitrogen desorption.

The N_2^* desorption yield function for $1N_2/50Kr$ is shown in Fig. 8(a) and the yield function of the luminescence emitted from a pure Kr film, taken from Ref. 16, is shown in Fig. 8(b) for a comparison. The photon signal in Fig. 8(b) exhibits a strong dependence on the electron energy with two regions of pronounced photon yield being discernible. The first peak has its onset at 10 eV, near the energy for exciting the first exciton in the Kr film.^{4,16} The second region, characterized by an onset near 20 eV, has been attributed to the excitation of two excitons due to multiple scattering.¹⁶ The decrease of the luminescence above 13 eV is due to the excitation of free-electron-hole pairs that have nonradiative relaxation channels (e.g., quenching at the film-metal interface).¹⁶ In Fig. 8(a), the N_2^* desorption signal exhibits a threshold at about 7.2 eV. Two further features can be recognized at 10.5 and 12.0 eV, followed by a peak with a maximum at 13.5 eV.

The shape of the N_2^* yield function in Fig. 8(a) is completely different from that of a pure 50-ML N_2 film [Fig. 1(b)], which exhibits a continuous increase in MP signal in the energy range 12–25 eV. The influence of the substrate Kr

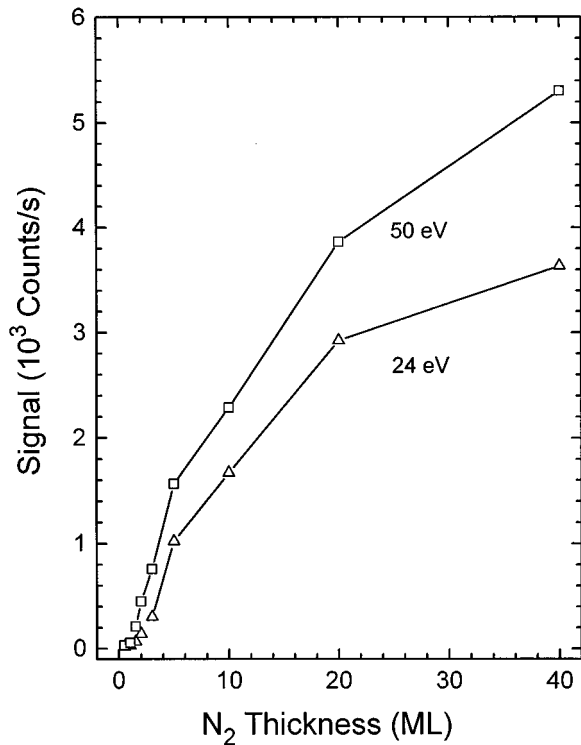


FIG. 7. N_2^* signal intensity as a function of N_2 thickness, deduced from Fig. 6.

film is obvious: the two curves in Fig. 8 have structures at 10.5 and 12 eV, with a minimum around 20 eV. These two curves also have different features. There is an obvious difference in the thresholds: 7.2 eV for N_2^* desorption from

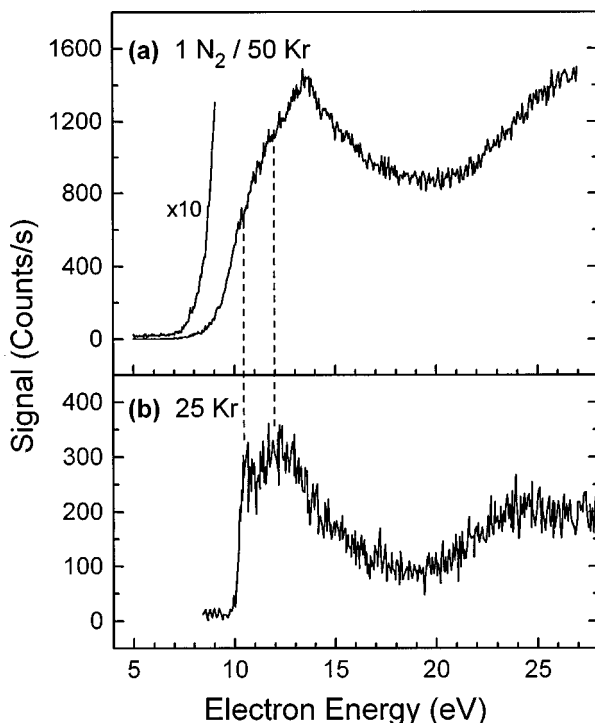


FIG. 8. (a) Yield function of electron-impact-stimulated N_2^* desorption from a 50-ML Kr film covered by 1 ML of N_2 ($1N_2/50Kr$). (b) Luminescence signal from a 25-ML Kr film produced by 8–28-eV electron impact (reproduced from Ref. 16).

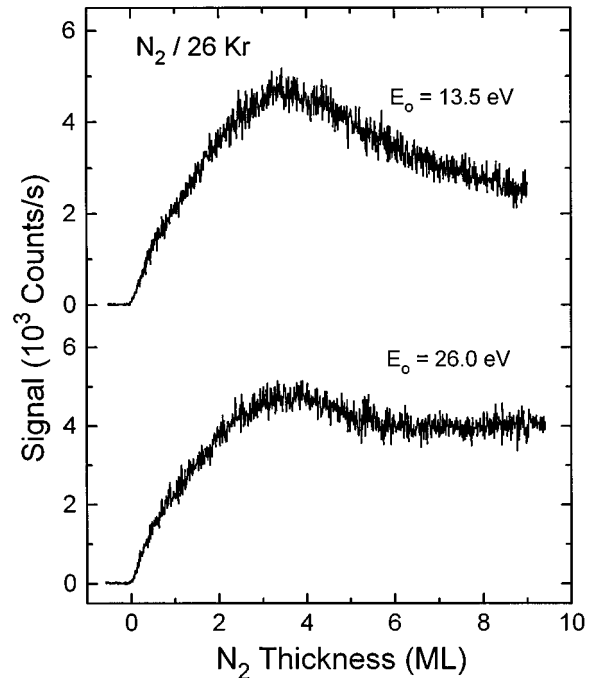


FIG. 9. N_2^* desorption yields induced by 13.5- and 26.0-eV electron impact and plotted as a function of thickness of N_2 layers adsorbed on a 26-ML Kr film.

$1N_2/50Kr$, which is much lower than the 10-eV threshold of the luminescence signal of a pure Kr film. An additional feature is present at 13.5 eV for $1N_2/50Kr$, and the relative signal intensity in the two main regions differs [e.g., the minimum is shallower for the curve in (a) than that in (b), and the intensity ratio at 25 eV to that at 12 eV is larger in (a) than in (b)]. Thus an additional contribution, which increases with electron energy, is present in (a).

Experiments similar to those performed with Xe spacer layers were also conducted on the thickness dependence of N_2^* desorption from N_2 deposited on Kr layers. The results for variable N_2 thicknesses on a 26-ML Kr film are shown in Fig. 9 for impact energies of 13.5 and 26.0 eV. Compared to the results in Fig. 4, the MP yield increases more sharply with N_2 coverage up to 1-ML N_2 , and then increases less and reaches a maximum at about 3.4-ML N_2 . The decrease observed for a higher coverage of N_2 is more pronounced for an impact energy of 13.5 eV.

The N_2^* desorption yield as a function of the thickness of Kr films is shown in Fig. 10. The yield increases rapidly with the thickness of Kr films for thickness below 9 ML, and has a tendency to saturate thereafter.

IV. DISCUSSION

From the dependence of the MP signal on the impact electron energy, we are able to identify the primary excitations which lead to desorption of metastable particles.^{22,23} For example, in Fig. 1(a) the enhancement in N_2^* desorption due to Xe has a maximum at an electron energy of 10 eV, which is near the maximum at 10 eV in Xe luminescence.^{16,23} An exciton in the Xe film is produced, and transfers its energy to N_2 molecules, as evidenced by an en-

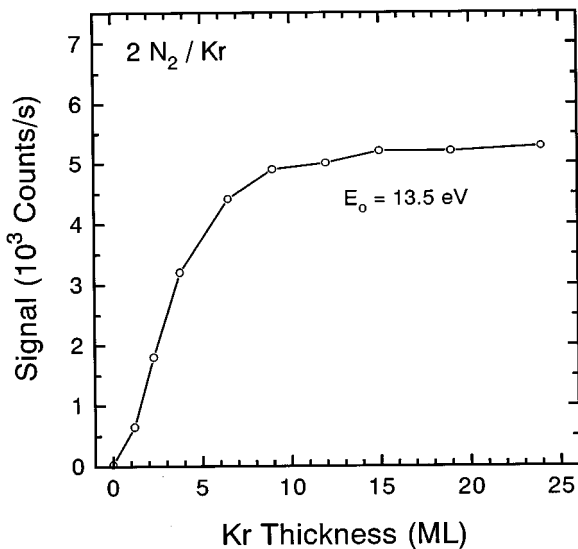


FIG. 10. The N_2^* desorption yield at an electron-impact energy of 13.5 eV displayed as a function of the thickness of a Kr spacer layer. 2 ML of N_2 were condensed on each Kr film.

ergy dependence of MP desorption characteristic of Xe luminescence.¹⁶ However, since N_2^* desorption is also observed from pure N_2 films [Fig. 1(b)], the contribution of desorption by direct excitation by the electron beam, which is expected to increase with incident energy, has to be considered as well. In fact, all our results can be explained by the interplay of these two desorption channels.

Consider N_2 molecules condensed on a RG (in our case Xe or Kr) film, as shown in Fig. 11. The yield of direct desorption (Y_d) and that induced by energy transfer (Y_t) are functions of the electron energy and the numbers of layers in both N_2 and RG films (T_{N_2} and T_{RG}). The total MP yield $Y = Y_d + Y_t$ then reflects changes in the intensity of either or both Y_d and Y_t . Factors including the excitation probability, electron-beam attenuation, exciton motion in the N_2 and RG films, energy-transfer efficiency, and desorption probability must be all considered. In doing so, Y_d and Y_t can be expressed as

$$Y_d = P_d n_d(N_2^*) \propto P_d \sum_{L=1}^{T_{N_2}} \{P_{N_2^*}[M_{N_2}, I_e(L)] f_{N_2}(L)\}, \quad (1)$$

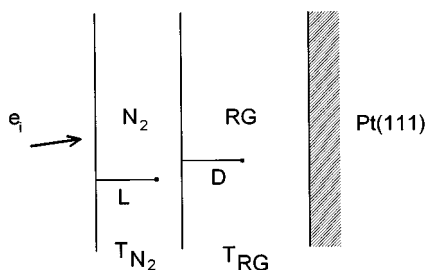


FIG. 11. Model for a N_2 -RG double-layer film condensed on Pt(111). e_i : incident electron beam. RG: rare-gas film (Xe or Kr). T_{N_2} : thickness of the N_2 film. T_{RG} : thickness of the RG film. L : distance within the N_2 film from the surface. D : distance within the RG film from the interface.

and

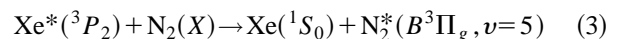
$$Y_t = P_d n_t(N_2^*) = P_d I_t f_{N_2}(T_{N_2}) n(RG^*)$$

$$\propto P_d I_t f_{N_2}(T_{N_2}) \sum_{D=1}^{T_{RG}} \{P_{RG^*}^* [M_{RG}, I_e(D, T_{N_2})] f_{RG}(D)\}, \quad (2)$$

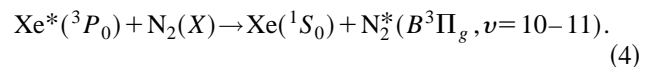
where P_d is the desorption probability of N_2^* at the surface during a given time interval, $n_d(N_2^*)$ and $n_t(N_2^*)$ are numbers of N_2^* present at the surface which are produced by direct excitation of N_2 or by energy transfer from RG excitons, respectively. Direct excitation means that the primary excitation occur in N_2 , including excitation of surface N_2 by N_2 bulk exciton which can transfer energy within the N_2 film. I_t is the sum of the transfer integrals between RG and N_2 excitons. $n(RG^*)$ is the amount of RG^* present at the N_2 -RG interface. $P_{N_2^*}$ and P_{RG^*} are excitation probabilities to form N_2^* and RG^* , which are functions of the electronic excitation matrix elements M and electron-beam intensity I_e . In a N_2 film, I_e depends on the distance L from the surface; in a RG film, I_e depends both on the distance D from the interface and the thickness of the adsorbed N_2 film. The exciton-motion function $f_{N_2}(L)$ or $f_{RG}(D)$ reflects the probability of the exciton to move to the surface, or the N_2 -RG interface in case of a RG exciton.

The desorption probability P_d is discussed first. A pure N_2 film is a special case of $T_{RG}=0$, where only direct desorption can be present, i.e., $Y \equiv Y_d$. The results for pure N_2 films [Figs. 1(b) and 6] show that the yield is very small for incident energy below 11.5 eV but increases above this energy. This is because P_d depends on the electronic states of N_2 . As we found in previous work,²² above 11.5 eV N_2 in the Rydberg state $E^3\Sigma_g^+$ desorbs as a result of cavity expulsion, a mechanism which produces much stronger yields than desorption via internal vibrational energy transfer from N_2 in the valence state $B^3\Pi_g$, which is the only state produced at lower energies. The desorption probability of $N_2^*(B)$ depends on the excitation of vibrational levels and the subsequent transfer of intramolecular vibrational energy to the molecule-surface bond.²⁵⁻²⁸ Mainly $N_2^*(B, \nu=1-5)$ can be excited by direct electron excitation in N_2 , according to gas-phase assignment,²⁹ whereas a different vibrational population results from energy transfer from rare gases.

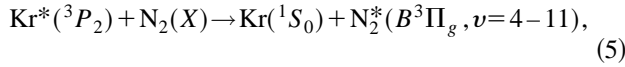
There exist experimental results and theoretical explanations for excitation energy transfer between Xe^* , Kr^* , and N_2 (Refs. 30 and 31) in the gas phase. Collisions at thermal energy are observed to produce vibrationally selective electronic-to-electronic energy transfer for near-resonant levels. For Xe, these reactions can be expressed as



and



For Kr, the situation is more complicated; collision between $Kr^*(^3P_2)$ and N_2 yields



but no N_2^* products are observed with $\text{Kr}^*(^3P_0)$, which reflects the lack of triplet acceptor states in the 10.5-eV range. $\text{N}_2^*(B)$ is the only metastable species observed by excitation energy transfer with Xe^* and Kr^* . Thus the interaction between N_2 and excitons derived from the atomic configurations $\text{Xe}^*(^3P_2)$ and $\text{Xe}^*(^3P_0)$, or $\text{Kr}^*(^3P_2)$ at the N_2 -RG interface, is expected to produce a B state by energy transfer in much higher vibrational levels than by direct electron impact. Since vibrational energy transfer to the molecule-surface bond at the film-vacuum interface is strongly dependent on the intramolecular vibrational quantum number,²⁷ P_d should be substantially larger when N_2^* is created via the energy-transfer mechanism. As seen in Fig. 1, below 11.5 eV, where desorption is only possible from vibrational energy exchange, desorption from a single layer of N_2 on a 50-ML Xe film produces a N_2^* yield one order of magnitude larger than those produced from a 50-ML N_2 film. A similar enhancement can be seen for the case of N_2 on Kr in Fig. 8(a) compared to Fig. 1(b).

Insight into the behavior of the exciton-motion function $f_{\text{N}_2}(L)$ can be acquired from the results on the thickness dependence of the MP signal from pure N_2 films (Fig. 7). Above two layers the influence of metal surface on N_2^* desorption appears to be relatively weak since a linear increase with T_{N_2} occurs from two to five layers (i.e., $Y_d \propto T_{\text{N}_2}$ for $2 \leq T_{\text{N}_2} < 5$ at constant incident energy E_0). Thus, according to Eq. (1), one can interpret this result as due to a yield directly proportional to the summation limit T_{N_2} with $P_{\text{N}_2^*}$ and $f_{\text{N}_2}(L)$ being independent of thickness. Furthermore, $f_{\text{N}_2}(L)$ is necessarily nonzero, and we must conclude that exciton motion exists in a pure N_2 film. The slower increase at above 5 ML is probably the result of electron-beam attenuation and/or a reduction in $f_{\text{N}_2}(L)$ since P_d is expected to remain the same. Since the signal does not saturate up to 40 ML of N_2 , we conclude that the mean exciton penetration depth is larger than 40 ML. The existence of exciton motion in a N_2 film is of primary importance in the following discussions, which are all based on this fact.

We have two cases of thickness-dependent experiments: case A, $T_{\text{RG}} = \text{const}$, with T_{N_2} increasing, and case B, $T_{\text{N}_2} = \text{const}$, with T_{RG} increasing. The results shown in Figs. 2, 3, and 4, as well as those in Fig. 9, belong to case A, and those in Figs. 5 and 10 to case B. We can predict from Eqs. (1) and (2) that, in case A, Y_d should increase with T_{N_2} , the same as in pure N_2 films, while Y_t should only increase up to a few layers of coverage as a result of increasing I_t , which is proportional to the number of molecules available for energy transfer. Beyond that coverage, I_t should remain constant with increasing N_2 thickness, but $f_{\text{N}_2}(T_{\text{N}_2})$ is expected to decrease due to the finite exciton penetration depth. Furthermore, the attenuation of the electron-beam intensity $I_e(D, T_{\text{N}_2})$ will reduce the primary excitations in RG films. In case B, obviously Y_d will remain constant, while Y_t will increase as a function of T_{RG} up to a thickness, where full

TABLE I. Behavior of the direct N_2^* desorption yield Y_d , the excitation energy transfer N_2^* desorption yield Y_t , and the total yield ($Y = Y_d + Y_t$) with increasing film thickness of molecular nitrogen (T_{N_2}) and rare gas (T_{RG}). Case A corresponds to $T_{\text{RG}} = \text{const}$ with T_{N_2} increasing, B to $T_{\text{N}_2} = \text{const}$ with T_{RG} increasing. +: increase, -: decrease, =: remains the same.

	Y_d	Y_t	Y
A	+, =	+, -	maximum may exist
B	=	+, =	reach a plateau

attenuation of the elastic beam and/or the RG exciton total penetration depth is reached. These behaviors are summarized in Table I.

We now return to results for N_2/Xe to point out that the MP desorption yield Y for $1\text{N}_2/50\text{Xe}$ resembles the electronic excitation function of Xe (i.e., P_{Xe^*}) and does not have the shape of Y_d (Fig. 1). We can therefore conclude that Y is dominated by the energy-transfer mechanism at low impact energies (i.e., Y_d does not contribute significantly to the signal), as established by Mann *et al.*²³ The same is true for low to intermediate T_{N_2} in Fig. 2, indicating that this is a strong desorption option. The minimum at around 16 eV in Figs. 1(a) and 2 should be less profound if there were any significant Y_d contribution around this energy. There is some Y_d contribution for $E_0 > 16$ eV, this can be deduced from Figs. 2 and 3, where Y_d accounts for a much shallower minimum at about 28 eV, and the overall increase of signal between 16 and 70 eV with increasing T_{N_2} . Thus, for $E_0 < 16$ eV, we have then $Y_t \gg Y_d$ with the total MP desorption $Y \approx Y_t$ for Xe. This condition applies to the curves $E_0 = 10$ eV in Fig. 4 and $E_0 = 10.3$ eV in the inset of Fig. 3, where the yield increases with T_{N_2} for small N_2 thickness as a result of an increase in the transfer probability I_t up to about 4 ML of N_2 . With a further increase of T_{N_2} , beam attenuation reduces the production of the Xe exciton and the decrease in $f_{\text{N}_2}(T_{\text{N}_2})$ further reduces the number of N_2^* arriving at the surface, hence Y_t . Thus a maximum is observed experimentally. At higher impact energies ($E_0 = 24$ eV in Fig. 4, and $E_0 = 50$ eV in the inset of Fig. 3), the Y_d contribution can no more be neglected: the increase in Y_d with T_{N_2} compensates for the decrease in Y_t , causing, instead of a maximum, a plateau for $E_0 = 24$ eV in Fig. 4, and a continual increase of Y as a function of T_{N_2} in Fig. 3. A similar behavior is observed for the N_2^* yield as a function of N_2 thickness on a 26-ML Kr film as seen in Fig. 9. In this case a maximum occurs before saturation for $E_0 = 26$ eV, indicating an overlap of Y_d and Y_t contributions in N_2/Kr double-layer films (see Table I, case A).

We want to point out that under conditions where the energy-transfer mechanism dominates, such as for $E_0 = 10.3$ eV in the inset of Fig. 3, one may be able to derive the $f_{\text{N}_2}(T_{\text{N}_2})$ value, from experimental results of a Y_t as a function of T_{N_2} using Eq. (2). Such a determination of the mean free path of excitons in the N_2 film, however, depends on the probability to form Xe^* which is also affected by the N_2 thickness, as expressed by $I_e(D, T_{\text{N}_2})$. By neglecting the influence of N_2 thickness on the Xe^* excitation and fitting the

data points for $T_{N_2} \geq 4$ in Fig. 3, a lower limit of 20 ML for the mean free path of N_2 excitons created by 10.3-eV electrons is obtained.

Case B is well represented by the results of Figs. 5 and 10: the MP yields increase and saturate as a function of T_{RG} (see Table I). The RG film thickness dependence of the N_2^* yield confirms the involvement of the energy-transfer mechanism in the desorption process. The signal saturates at lower thicknesses in the case of a Xe substrate film, indicating a difference in the behavior of the function $n(RG^*)$ in Eq. (2) (i.e., the density of the exciton for energy transfer at the N_2 -RG interface reaches a maximum around 10 ML in the case of Kr, and around 3 ML in the case of Xe). We now further examine the differences between Xe and Kr in the region $E_0 < 16$ eV, where the energy-transfer mechanism dominates the MP desorption in the N_2 /Xe system.

Comparing Figs. 1(a) and 8(a) for the N_2^* yield from $1N_2/50Xe$ and $1N_2/50Kr$, it is obvious that the MP yield function depends strongly on the kind of RG solid on which the diatomic molecules are adsorbed. This fact per se provides strong evidence of the involvement of RG solids in MP desorption, as proposed by Mann *et al.*²³ For 1-ML N_2 on a 50-ML Kr film, if MP desorption were to proceed only via excitation energy transfer from excitons in Kr film to the adsorbed molecules, the MP yield functions would have the same energy dependence as the Kr luminescence, as it is the case for the $1N_2/50Xe$ film. Indeed, a coarse similarity is observed for the $1N_2/50Kr$ double-layer film, as shown in Figs. 8(a) and 8(b), but the observed differences suggest considerable contribution from direct desorption with $Y_t \geq Y_d$. The identical desorption threshold of 7.2 eV for $1N_2/50Kr$ and the pure 50-ML N_2 film [Figs. 8(a) and 1(b)] indicates that primary excitation of N_2 to the $B^3\Pi_g$ state also contributes to N_2^* desorption from $1N_2/50Kr$. The two features at 10.5 and 12.0 eV in the yield function for $1N_2/50Kr$ [Fig. 8(a)] can easily be assigned to the energy-transfer mechanism, based on the fact that these two maxima are also observed in Fig. 8(b) for Kr luminescence. The broad maximum at 14.5 eV for the pure N_2 film is shifted to lower energy in the yield function for $1N_2/50Kr$, giving a maximum at 13.5 eV from the Y_d contribution.

The differences in Y_d and Y_t contributions for MP desorption from Xe and Kr substrate films may come from one or both of the following possibilities: first, Kr compared to Xe may have a lower efficiency for transferring its excitation energy to adsorbates [i.e., the sum of the transfer integrals has a smaller magnitude for Kr giving $I_t(Kr) < I_t(Xe)$]. Hence according to Eq. (2) $Y_t(Kr) < Y_t(Xe)$ and the effect of the Y_d contribution become more visible from Kr than from Xe substrates even if Y_d is the same in both cases. That would mean that on a covered Xe film, Y_d is present, but its contribution is overwhelmed by the energy-transfer mechanism. Second, the directly excited state of the adsorbates may be quenched in the presence of Xe, such that $Y_d(Xe) < Y_d(Kr)$. We believe

that these two factors work together to produce the observed differences in yields between Kr and Xe. A similar trend has been observed in low-energy electron-induced anion desorption, where anion yields were found to be enhanced for RG solids covered with simple molecules as the result of energy and charge transfer from the RG to the adsorbate.³² The enhancement (i.e., the transfer efficiency) was found to be on the order of $Xe > Kr \gg Ar$. Above the energy of enhancement, quenching of the direct signal was observed in the same experiment, again on the order of $Xe > Kr \gg Ar$.

Further support of our hypothesis comes from gas-phase data. The quenching rate constant of Kr^* in N_2 is smaller than that for Xe^* in N_2 . For $Kr^*(^3P_2)$, it is only 0.41×10^{-11} cm^3/s , while that for $Xe^*(^3P_2)$, it has been measured to lie in the range $1.9-2.48 \times 10^{-11}$ cm^3/s .^{31,33,34} Since $N_2^*(B)$ is the only product in both cases,^{30,31} the quenching rate constant is equivalent to the formation rate constant of $N_2^*(B)$. Assuming that in our films the energy transfer between a Xe (Kr) exciton and N_2 proceeds in a manner similar to a gas-phase collision, as proposed by Mann *et al.*,²³ $N_2^*(B)$ formation via energy transfer should be more effective on a Xe than on a Kr substrate. This is particularly true of $Kr^*(^3P_0)$ which has a very low quenching rate in N_2 and produces no N_2^* products.³¹ The Y_t contribution is therefore expected to be larger for Xe than for Kr, in support of our experimental finding.

V. CONCLUSIONS

We presented a detailed analysis of low-energy-electron-stimulated desorption of metastable particles for N_2 layers adsorbed on Kr and Xe multilayer films. The N_2^* desorption yields were found to depend on the direct excitation of electronic states in the N_2 adsorbate film by the incident electron beam, and on electronic energy transfer from the rare gas to the adsorbate. The two contributions vary in magnitude with electron energy and the respective thicknesses of the double-layer systems. Energy transfer dominates MP desorption in N_2 /Xe double-layer films at low electron energy ($E_0 \leq 16$ eV) and low-to-intermediate N_2 thickness ($T_{N_2} \leq 4$ ML), whereas in the N_2 /Kr systems, both the direct and energy-transfer mechanisms contribute substantially to the total N_2^* yields. For both systems, the direct desorption contribution increases with electron energy, and is observed from Kr films even at very low electron energies. The differences in the behavior of the desorption yields between N_2 /Kr and N_2 /Xe films has been ascribed mainly to the higher efficiency for energy transfer from excitons in Xe films to adsorbed N_2 molecules than from those in Kr films.

ACKNOWLEDGMENT

This work was sponsored by the Medical Research Council of Canada.

- ¹N. Schwentner and E. E. Koch, Phys. Rev. B **14**, 4687 (1976); M. E. Fajardo and V. A. Apkarian, J. Chem. Phys. **89**, 4102 (1988).
- ²E. P. Marsh, T. L. Gilton, W. Meier, M. R. Schneider, and J. P. Cowin, Phys. Rev. Lett. **61**, 2725 (1988); St. J. Dixon-Warren, J. C. Polanyi, C. D. Stanners, and G.-Q. Xu, J. Phys. Chem. **94**, 5664 (1990); S. K. Jo and J. M. White, *ibid.* **94**, 6852 (1990).
- ³Z. Lu, M. T. Schmidt, D. V. Podlesnik, C. F. Yu, and R. M. Osgood, Jr., J. Chem. Phys. **93**, 7951 (1990); Y. Chen, J. M. Seo, F. Stepniak, and J. H. Weaver, *ibid.* **95**, 8442 (1991); F. Bozso and Ph. Avouris, Phys. Rev. B **44**, 9129 (1991).
- ⁴P. Feulner and D. Menzel, in *Laser Spectroscopy and Photochemistry on Metal Surfaces*, edited by H.-L. Dai and W. Ho (World Scientific, Singapore, 1995).
- ⁵I. Ya. Fugol, Adv. Phys. **27**, 1 (1978).
- ⁶N. Schwentner, E.-E. Koch, and J. Jortner, in *Electronic Excitations in Condensed Rare Gases*, edited by G. Höhler (Springer, Berlin, 1985).
- ⁷G. Zimmerer, in *Excited-State Spectroscopy in Solids*, edited by U. M. Grassano and N. Terzi (North-Holland, Amsterdam, 1987).
- ⁸T. Kloiber, H.-J. Kmiciek, M. Kruse, M. Schreiber, and G. Zimmerer, J. Lumin. **40&41**, 593 (1988).
- ⁹A. Hourmatallah, F. Colletti, and J. M. Debever, J. Phys. C **21**, 1307 (1988).
- ¹⁰F. Coletti, J. M. Debever, and G. Zimmerer, J. Phys. (Paris) Lett. **45**, 467 (1984).
- ¹¹F. Coletti, J. M. Debever, and A. Hourmatallah, Phys. Scr. **35**, 168 (1987).
- ¹²T. Kloiber, W. Laasch, G. Zimmerer, F. Coletti, and J. M. Debever, Europhys. Lett. **7**, 77 (1988); T. Kloiber and G. Zimmerer, Radiat. Eff. Defects Solids **109**, 219 (1989); T. Kloiber and G. Zimmerer, Phys. Scr. **41**, 962 (1990).
- ¹³C. T. Reimann, W. L. Brown, D. E. Grosjean, and M. J. Nowakowski, Phys. Rev. B **45**, 43 (1992).
- ¹⁴C. T. Reimann, W. L. Brown, and R. E. Johnson, Phys. Rev. B **37**, 1455 (1988).
- ¹⁵E. Hudel, E. Steinacker, and P. Feulner, Phys. Rev. B **44**, 8972 (1991).
- ¹⁶A. Mann, G. Leclerc, and L. Sanche, Phys. Rev. B **46**, 9683 (1992).
- ¹⁷D. J. O'Shaughnessy, J. W. Boring, S. Cui, and R. E. Johnson, Phys. Rev. Lett. **61**, 1535 (1988); I. Arakawa, M. Takahashi, and K. Takeuchi, J. Vac. Sci. Technol. A **7**, 2090 (1989); I. Arakawa and M. Sakurai, in *Desorption Induced by Electronic Transitions, DIET IV*, edited by G. Betz and P. Varga (Springer, Berlin, 1990), p. 246.
- ¹⁸G. Leclerc, A. D. Bass, M. Michaud, and L. Sanche, J. Electron Spectrosc. Relat. Phenom. **52**, 725 (1990).
- ¹⁹G. Leclerc, A. D. Bass, A. Mann, and L. Sanche, Phys. Rev. B **46**, 4865 (1992).
- ²⁰D. E. Weibel, A. Hoshino, T. Hirayama, M. Sakurai, and I. Arakawa, in *Desorption Induced by Electronic Transitions, DIET V*, edited by A. R. Burns, E. B. Stechel, and D. R. Jennison (Springer, Berlin, 1993), p. 333; D. E. Weibel, T. Hirayama, and I. Arakawa, Surf. Sci. **283**, 204 (1993).
- ²¹S. Cui, R. E. Johnson, and P. T. Cummings, Phys. Rev. B **39**, 9580 (1989); W. T. Buller and R. E. Johnson, *ibid.* **43**, 6118 (1991).
- ²²H. Shi, P. Cloutier, and L. Sanche, Phys. Rev. B **52**, 5385 (1995).
- ²³A. Mann, P. Cloutier, D. Liu, and L. Sanche, Phys. Rev. B **51**, 7200 (1995).
- ²⁴E. E. Eyler and F. M. Pipkin, J. Chem. Phys. **79**, 3654 (1983); H. A. van Sprang, G. R. Möhlmann, and F. J. de Heer, Chem. Phys. **24**, 429 (1977); S. Shadfar, S. R. Lorentz, W. C. Paske, and D. E. Golden, J. Chem. Phys. **76**, 5838 (1982).
- ²⁵D. Lucas and G. E. Ewing, Chem. Phys. **58**, 385 (1981).
- ²⁶H. J. Kreuzer and D. N. Lowy, Chem. Phys. Lett. **78**, 50 (1981); Z. W. Gortel, H. J. Kreuzer, P. Piercy, and R. Teshima, Phys. Rev. B **27**, 5066 (1983); **28**, 2119 (1983); H. J. Kreuzer and Z. W. Gortel, *ibid.* **29**, 6926 (1984).
- ²⁷F. Dzegilenko, E. Herbst, and T. Uzer, J. Chem. Phys. **102**, 2593 (1995), and citations therein; E. Galloway and E. Herbst, Astron. Astrophys. **287**, 633 (1994).
- ²⁸B. Fain and S. H. Lin, Chem. Phys. Lett. **114**, 497 (1985); B. Fain, *ibid.* **118**, 283 (1985).
- ²⁹P. Hammond, G. C. King, J. Jureta, and F. H. Read, J. Phys. B **20**, 4255 (1987).
- ³⁰D. H. Stedman and D. W. Setser, J. Chem. Phys. **52**, 3957 (1970); T. Krümpelmann and Ch. Ottinger, Chem. Phys. Lett. **140**, 142 (1987); J. Chem. Phys. **88**, 5245 (1988); M. Tsuji, K. Yamaguchi, and Y. Nishimura, Chem. Phys. **125**, 337 (1988); L.-Y. C. Chiu, Y.-N. Chiu, T. Krümpelmann, and Ch. Ottinger, Chem. Phys. Lett. **151**, 220 (1988), **157**, 60 (1989); W. Böhle, H. Geisen, T. Krümpelmann, and Ch. Ottinger, Chem. Phys. **133**, 313 (1989); V. Aquilanti, R. Candori, P. Pirani, T. Krümpelmann, and Ch. Ottinger, *ibid.* **142**, 47 (1990), V. Aquilanti, R. Candori, P. Pirani, and Ch. Ottinger, *ibid.* **187**, 171 (1994); T. G. Aardema, E. J. van Nijnatten, and H. C. W. Beijerinck, *ibid.* **184**, 273 (1994).
- ³¹C. J. Tracy and H. J. Oskam, J. Chem. Phys. **65**, 166 (1976); N. Sadeghi and D. W. Setser, Chem. Phys. Lett. **82**, 44 (1981); M. Tsuji, K. Yamaguchi, and Y. Nishimura, J. Chem. Phys. **89**, 3391 (1988); R. Sobczynski, R. Beaman, D. W. Setser, and N. Sadeghi, Chem. Phys. Lett. **154**, 349 (1989); R. Sobczynski and D. W. Setser, J. Chem. Phys. **95**, 3310 (1991).
- ³²P. Rowntree, L. Parenteau, and L. Sanche, Chem. Phys. Lett. **182**, 479 (1991); P. Rowntree, H. Sambe, L. Parenteau, and L. Sanche, Phys. Rev. B **47**, 4537 (1993).
- ³³J. E. Velazco and D. W. Setser, Chem. Phys. Lett. **25**, 197 (1974); J. E. Velazco, J. H. Kolts, and D. W. Setser, J. Chem. Phys. **69**, 4357 (1978).
- ³⁴C. J. Tracy, R. C. Brindle, and H. J. Oskam, J. Chem. Phys. **68**, 4321 (1978).